Single and multiple ionization of C_{60} fullerenes and collective effects in collisions with highly charged C, F, and Si ions with energy 3 MeV/u

A. H. Kelkar,[1,*] U. Kadhane,[1] D. Misra,[1] L. Gulyas,[2] and L. C. Tribedi[1]
[1]*Tata Institute of Fundamental Research, Mumbai, India*
[2]*ATOMKI, Debrecen, Hungary*
(Received 19 February 2010; published 27 October 2010)

We have measured absolute cross sections for single, double, triple, and quadruple ionization of C_{60} in collisions with 3 MeV/u C, F, and Si projectile ions at various projectile charge states. The experiment was performed using the recoil-ion time-of-flight technique. Projectile charge state dependence of the ionization yields was compared mainly with a model based on the giant dipole plasmon resonance (GDPR). In some cases, the continuum-distorted-wave–eikonal-initial-state (CDW-EIS) model which is normally applied for ion-atom collisions was also used as a reference. An excellent qualitative agreement between the experimental data for single and double ionization and the GDPR model predictions was found for all projectile charge states.

DOI: 10.1103/PhysRevA.82.043201 PACS number(s): 36.40.−c, 34.50.Fa, 61.46.−w

I. INTRODUCTION

Collisional interactions of the C_{60} fullerene with fast and slow highly charged heavy ions, electrons, and photons have been the focus of atomic physics research for a couple of decades now. In basic atomic physics research, C_{60} is viewed as a model system for understanding the interactions of mesoscopic many-body systems with photons [1] and charged particles. A C_{60} molecule has solidlike electron density [2], which offers a unique possibility to explore the collective properties on a microscopic scale. The delocalization of the valence π electrons in a C_{60} molecule gives rise to a collective mode of oscillation called the giant dipole plasmon resonance (GDPR). The resonance is very similar to the nuclear giant dipole resonance and the plasma oscillations in solids [3]. The resonance peaks at energy of 20 eV with a full width at half maximum (FWHM) of 10 eV, and it has an oscillator strength of 71 [4]. The effect of this collective excitation on the Lyman x-ray production cross section following electron capture from C_{60} has been reported by Kadhane *et al.* [5]. The intense laser-induced multiphoton ionization of fullerenes has also been investigated [6], and it was shown that both single and double ionization of C_{60} were fully dominated by the plasmon excitation. In the field of the ion-C_{60} collision, there are several studies [7–11] which deal with the influence of collective excitation on the ionization of C_{60}. LeBrun *et al.* reported the first such studies and interpreted their results on single ionization of C_{60} on the basis of a plasmon excitation model [7]. This model predicts a weak projectile velocity (v_p) dependence of the plasmon excitation probability, but a strong dependence on q_p (projectile charge state). Earlier investigations [10,11] showed that single plasmon excitation accounts for about 50% of the single-ionization cross section. Previously, we investigated the effect of the projectile charge state on the single-, double- [12], and triple-ionization [13] cross section of C_{60} under heavy-ion impact, and the data was analyzed within the framework of the GDPR model. However, the experiments were restricted to the measurement of relative ionization cross sections, and hence a quantitative comparison could not be presented. In addition, the atomic number dependence was not studied either.

Here, we present an extensive study on the absolute cross sections of single and multiple ionization of C_{60} and its dependence on the Coulomb perturbation strength ($S = q_p/v_p$) of the heavy-ion projectile. The perturbation strength was varied between 0.4 and 1.3 by changing the charge state of the projectile ions at a constant beam velocity. The results are compared with the calculations based on the GDPR model. In some cases, we used the continuum-distorted-wave–eikonal-initial-state (CDW-EIS) model, which is an *ab initio* quantum-mechanical model for ion-atom collision [14,15].

II. EXPERIMENT

The projectile-ion beams were obtained from the 14 MV tandem Pelletron accelerator facility at Tata Institute of Fundamental Research (TIFR), Mumbai. The projectile energy was fixed at 3 MeV/u. The primary projectile beam was made to pass through a postacceleration carbon foil stripper to obtain different charge states, which were then analyzed using a switching magnet. The beam was collimated to 2×2 mm^2 using a pair of four jaw slits placed 1 m apart from each other. The projectile beams used in this study were C^{q_p+}, F^{q_p+}, and Si^{q_p+}, with q_p varying between 4 and 14. A typical beam current of 1–3 nA was used which was measured on a Faraday cup placed downstream, i.e., after passing through the C_{60} vapor jet. For target preparation, commercially available C_{60} powder of 99.9% purity was heated in a temperature-controlled stainless steel oven at 400°C, and an effusive beam of C_{60} vapor was introduced in the interaction zone through a nozzle of diameter 2 mm. The recoil ions were mass analyzed using a Wiley-McLaren [16] type time-of-flight (TOF) mass spectrometer placed orthogonal to the ion beam and the fullerene jet. Vacuum in the scattering chamber was better than 5×10^{-7} mbar. Figure 1 shows a schematic diagram of the TOF setup. The extracted ions were detected using a microchannel plate (MCP) detector placed at the end of the flight tube having an effective detection diameter of 40 mm. On the electron side, a 10×1.5 mm slit was placed in front of the pusher plate to reduce excessive electron count rate

*lokesh@tifr.res.in

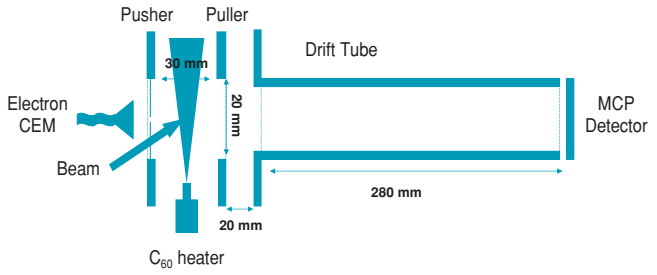

FIG. 1. (Color online) Schematic drawing of the TOF mass spectrometer.

at the channel electron multiplier (CEM) placed behind the pusher plate. The signal from the electron CEM was used as a start trigger, and the signal from the MCP was used as a stop trigger to generate the TOF spectra. To obtain absolute cross sections, it was necessary to correct the measured TOF spectrum for collection efficiency of the spectrometer and detection efficiency of the MCP detector. For a given geometry, the collection efficiency of a TOF mass spectrometer depends on the electric fields in the extraction and acceleration regions as well as on the kinetic energy of the recoil ions. Ion trajectory simulations performed using the SIMION code showed that for an extraction field of 330 V/cm, collection efficiency of our TOF mass spectrometer was 100% (excluding attenuation due to the wire mesh) for all the ions having kinetic energy less than 5 eV. Detection efficiency of the MCP detector was calculated using an empirical relation developed by Itoh *et al.* [10] for positively charged C_{60} ions. The efficiency is given by

$$\epsilon = 1 - e^{[-(1.48E+2.18E^2)/100]}, \tag{1}$$

where E is the energy of the C_{60} ions in keV. A comparison of the experimentally measured efficiencies with the above relation has been reported elsewhere [17]. Errors in the relative cross-section measurement were estimated by taking into account the small temperature fluctuation (~5°C) of the C_{60} oven during a given run. Several runs were repeated at a constant temperature, and the relative yields were found to be reproduced within 10%. Relative error in the cross section was, therefore, estimated to be approximately 10%. However, for $C_{60}{}^{4+}$ ions, the uncertainty in the yield was more (~15%) due to statistical error and the multiple peak fitting procedure [13] adopted.

The data on the absolute cross sections for charged particle induced ionization of C_{60} are very rare in the literature, and the absolute cross sections have been estimated, mainly using the vapor pressure data for C_{60} as reported by Abrefah *et al.* [18]. For example, Itoh *et al.* [10,11] measured the absolute cross sections for single and double ionization of C_{60} under fast proton and electron impact. In the present study, we have used a different approach to calculate the absolute ionization cross sections. Normalization of the relative cross sections was done in two steps. In the first step, we measured the total ionization cross section of C_{60} in collisions with 4 MeV/u F^{9+} projectile ions. This was done by measuring the energy and angular distributions of the double differential cross sections (DDCSs) of continuum electrons including the *K-LL* Auger electrons for C_{60} in an angular range of 30°–150°. The e^--DDCSs were measured in a separate experiment using an electrostatic hemispherical analyzer. The *K-LL* Auger e^--DDCSs for a methane target were also measured in the same experiment to obtain the absolute *K-LL* Auger emission cross section for carbon from the first-principle calculation under static gas pressure conditions, as described elsewhere [19,20]. The absolute cross section thus obtained for carbon *K-LL* Auger emission was then used to normalize the continuum part of the e^--DDCS spectrum obtained for C_{60} by normalizing the *K-LL* Auger yields of C_{60} to that obtained for the methane target. Further, the absolute total ionization cross section was obtained by integrating the e^--DDCS over the entire energy and angular range. Details of the experiment for e^--DDCS measurements will be published elsewhere, since it was aimed for a different study.

In the second step, we normalized the total recoil-ion yield deduced from the TOF mass spectrum (for the 3 MeV/u F^{9+} projectile) to the total ionization cross section obtained from the DDCS measurements. The necessary energy scaling of the *K*-ionization cross section from 4 to 3 MeV/u projectile beam energy was also done.[1] The main sources of uncertainty in the absolute cross-section measurement were the estimation of the absolute *K-LL* Auger emission cross section for methane (~10%) and the relative *K-LL* Auger cross-section measurement for C_{60} (~20%). After accounting for the uncertainties in the C_{60} vapor density fluctuations (10%) and normalization factors, the total error in absolute ionization cross section was estimated to be about 30%.

III. THEORETICAL MODEL

Various theoretical models can be invoked to describe the ionization of C_{60} by a fast heavy-ion projectile. In this study, we have compared our experimental results with two theoretical models, namely, the GDPR model [7] and the CDW-EIS model. In the GDPR model, the Coulomb field of a projectile ion excites surface plasmons in a C_{60} molecule and the effective number of plasmons generated is given by

$$N(b) = \int dE \frac{f(E)}{E} \frac{2q_p^2 e^4}{mv^2} \frac{1}{b^2} \left(\xi^2 K_1^2(\xi) + \frac{1}{\gamma^2} \xi^2 K_0^2(\xi) \right), \tag{2}$$

where $\xi = Eb/\gamma\hbar v$, $f(E)$ is the oscillator strength distribution function, b is the impact parameter, and q_p is the projectile charge state. The plasmon excitation cross section is then obtained by integrating $N(b)$ over all impact parameters as follows:

$$\sigma_{\rm pl} = 2\pi \int_0^\infty db\, bN(b) \exp[-N(b)]. \tag{3}$$

Unlike the GDPR model, which involves collective behavior, the CDW-EIS model is an *ab initio* quantum-mechanical approach for ion-atom collision. The model has been applied

[1]The energy scaling was done using a well-known model, the ECPSSR [21] for inner-shell ionization. The model is based on a perturbed-stationary state (PSS) approximation, and it includes the energy-loss (E) effect, the Coulomb (C) deflection effect, and the relativistic (R) wave-function corrections. It is known to very well reproduce the energy dependence of *K*-ionization cross sections under heavy-ion collisions.

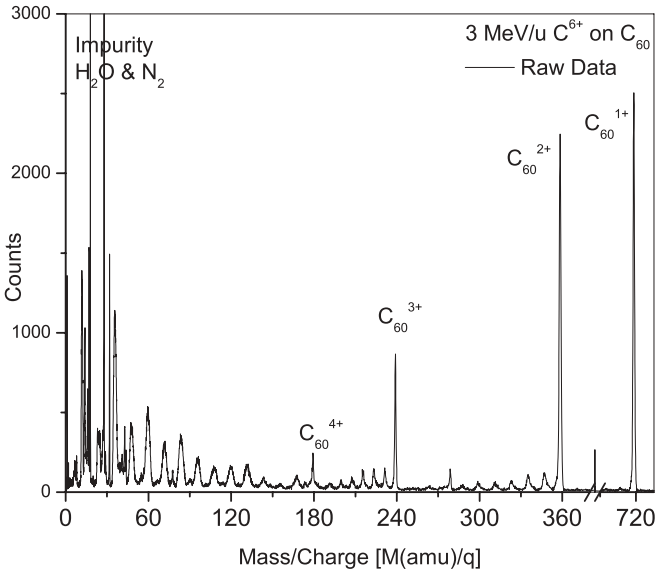

FIG. 2. TOF mass spectrum of the recoil ions showing the single and multiple ionization and fragmentation products of C_{60} in collisions with for 3 MeV/u C^{6+} ions. The TOF of the recoil ions has been converted to their mass-to-charge ratio (x axis). The mass peaks are not corrected for MCP detection efficiency. Also visible in the spectrum are the peaks corresponding to N_2 and H_2O present in the background gas.

for heavy-ion collisions with carbon atoms where the initial-state wave function of the carbon atom has been modified to include the electron density profile of a C_{60} molecule. In this sense the CDW-EIS model can be applied to a C_{60} target only to obtain a crude estimation of the ionization cross section.

IV. RESULTS AND DISCUSSIONS

Figure 2 shows a typical raw TOF mass spectrum of C_{60} in collisions with a C^{6+} ion beam. The time-of-flight has been converted into mass-to-charge ratio for identification of the various fragmentation products. Figure 3 shows the same spectrum corrected for the MCP detection efficiency.

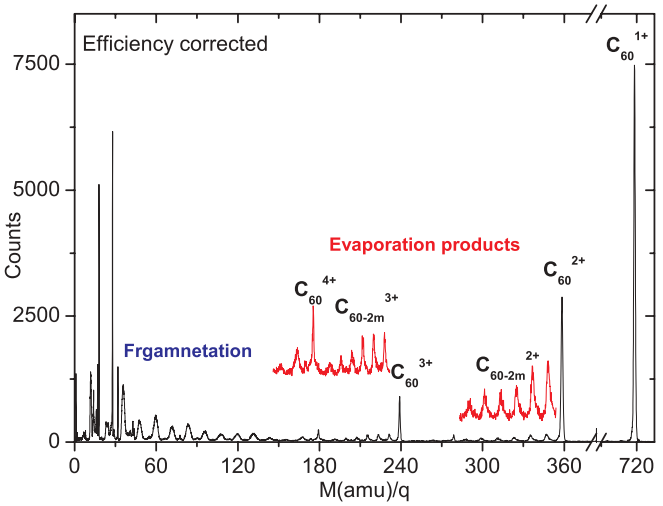

FIG. 3. (Color online) Same TOF spectrum as in the Fig. 2, corrected for MCP detection efficiency.

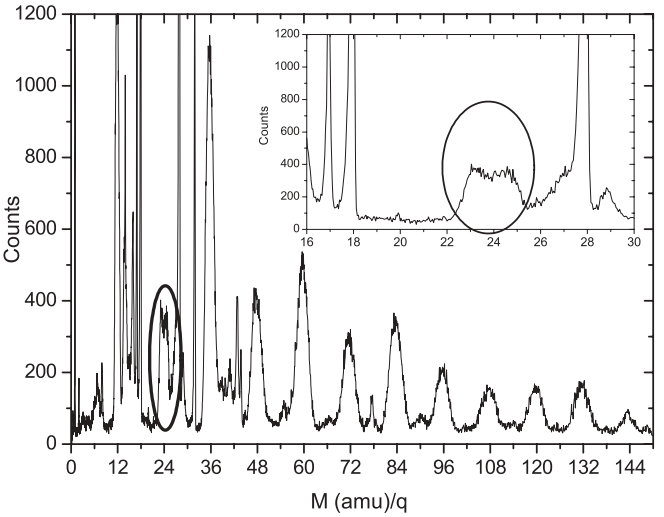

FIG. 4. Expanded view of low mass region in Fig. 3. Singly ionized C_n^{1+} cluster ions can be seen for $n = 1$ to 12. Inset in the figure shows peculiar structure of C_2^{1+} fragment ion peak observed in the experiment.

The resolution of the mass spectrometer ($\triangle m/m$) was found to be better than 1 in 130. Several studies on collision of C_{60} with fast and slow highly charged ions have established characteristic features of the TOF spectrum which can be broadly divided into three regions: (i) the intact $C_{60}^{q_r+}$ cages with different charge states which are visible as the most prominent peaks; (ii) the evaporation peaks $C_{60-2m}^{q_r+}$, which result from evaporation of neutral C_2 units from $C_{60}^{q_r+}$; and finally (iii) the small C_n^+ fragments (on left side of the spectrum), which mainly result from an almost complete destruction of the C_{60} cage. In Fig. 4, we have shown the enlarged view of the fragmentation region. One can easily see that the peak shape of the C_2^+ mass fragment is very different from the rest of the peaks. It has a plateau region in the middle, and its FWHM is almost double the width of other fragmentation peaks. This feature is attributed to the existence of two different channels for C_2^+ ion production. A direct fragmentation channel in which the kinetic energy release is around 3–4 eV [11] and a superasymmetric fission channel, in which the kinetic energy of emitted C_2^+ ions is around 5–10 eV [22]. Since the collection efficiency of our TOF spectrometer is 100% only for ions with kinetic energies up to 5 eV, a fraction of C_2^+ ions which are emitted at an angle close to 90° to the spectrometer axis are not collected. This is the reason for the plateau in the C_2^+ fragment peak. Larger kinetic energy release in superasymmetric fission process also explains the broadening of the C_2^+ peak compared to other fragmentation peaks.

In Fig. 5, we have plotted the single-, double-, triple-, and quadruple-ionization cross sections of C_{60} (on absolute scale) as a function of q_p. These data are shown in Table I. Note that the data for all three projectile ion species, namely, C, F, and Si are plotted on the same scale in each block and no normalization has been done. The single- and double-ionization cross sections scale linearly with q_p over the entire range of projectile charge, i.e., from $q_p = 4$ to 14. Respective plasmon excitation cross sections calculated using the GDPR

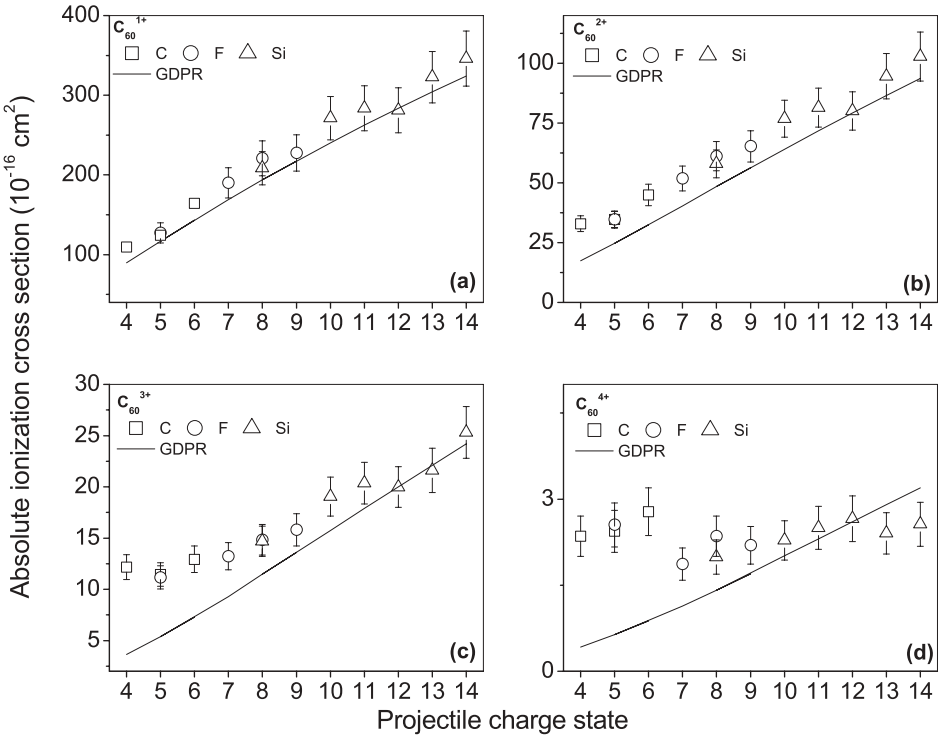

FIG. 5. Absolute ionization cross sections for (a) single, (b) double, (c) triple, and (d) quadruple ionization of C_{60} in collisions with 3 MeV/u C, F, and Si projectiles. Solid lines show the respective GDPR predictions. The GDPR curve is normalized to the experimental data at 12+ projectile charge state in each case, and the respective normalization factors are as follows (a) 1.9, (b) 1.9, (c) 1, and (d) 0.22.

model are also plotted in each block for comparison. The cross sections from the GDPR model have been normalized at one point in each case. The normalization factor is about 1.9 for single and double ionization [Figs. 5(a) and 5(b)]. This normalization is suitable for investigating the extent of qualitative agreement between the data and the GDPR model. One can see that in the case of single and double ionization, the experimental and theoretical slopes are in excellent agreement. Even though the normalization for each recoil-ion charge state is arbitrarily done at one point, it is important to note that the normalization factors are the same for single and double ionization. This implies that for single and double ionization, the GDPR cross sections are almost 50% of the experimental values. This certainly indicates the dominant role of the GDPR on single- and double-ionization processes. Cheng *et al.* [8] and Itoh *et al.* [11] have also reported that the GDPR process accounts for almost half the measured single- and double-ionization cross sections using highly charged Xe and H^+ projectiles, respectively. The qualitative as well as quantitative agreement between the present investigation and these earlier reports is very encouraging, especially, in light of the very different normalization technique applied in the present study to obtain the absolute cross sections.

TABLE I. Absolute cross sections for single, double, triple, and quadruple ionization of C_{60} in collisions with 3 MeV/u C, F, and Si projectiles.

Charge state	C_{60}^{1+}	C_{60}^{2+} (10^{-16} cm^2)	C_{60}^{3+}	C_{60}^{4+}
		Projectile - carbon		
4	109	33	12.2	2.35
5	124	35	11.4	2.44
6	164	45	12.9	2.79
		Projectile - fluorine		
5	127	35	11.2	2.55
7	189	52	13.2	1.87
8	221	61	14.8	2.35
9	227	65	15.8	2.2
		Projectile - silicon		
8	208	58	14.6	1.98
10	271	77	19.0	2.28
11	283	81	20.3	2.5
12	281	80	20.0	2.66
13	323	95	21.6	2.4
14	346	102	25.3	2.56

The behavior of the triple-ionization cross section [Fig. 5(c)] is different from that for the single- and double-ionization yields. At low q_p, its dependence on projectile charge state is very weak, whereas a linear dependence is seen for higher projectile charge states ($q_p \geqslant 9$). The normalization factor for the GDPR cross sections is also close to unity in the case of triple-ionization yields. Nevertheless large deviations are visible between the data and the GDPR values for low projectile charge states. The quadruple-ionization cross sections shown in Fig. 5(d) show no appreciable dependence on q_p and any comparison with the GDPR model is not possible. Further, the GDPR model highly overestimates the measured cross sections, which is evident from the normalization factor [see caption for Fig. 5(d)]. This behavior is expected, since the GDPR model is purely based on a perturbative approach which is applicable to only large impact parameter collisions [7,13]. The deviations from the GDPR model at low q_p and for higher recoil-ion charge states (C_{60}^{3+}, C_{60}^{4+}) are possibly due to the increased importance of the low impact parameter processes such as evaporation and fragmentation.

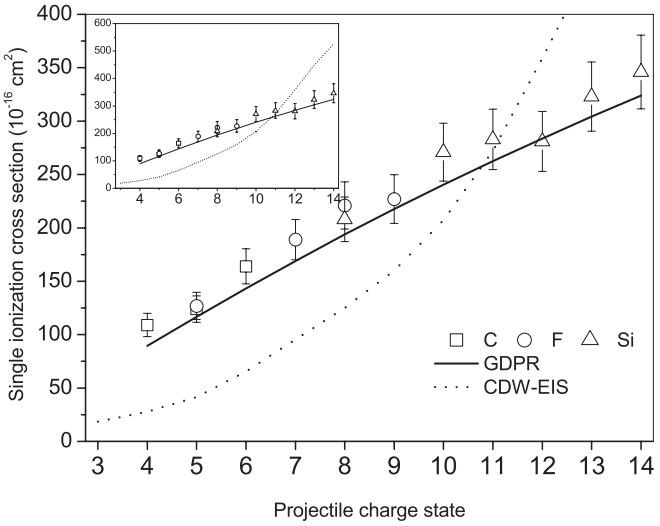

FIG. 6. Absolute single-ionization cross sections for C_{60} in collisions with 3 MeV/u C, F, and Si projectile ions. Open symbols show the experimental data. The solid line represents the normalized GDPR cross sections (see caption for Fig. 5). The dotted line shows the single-ionization cross sections calculated using CDW-EIS calculations for a carbon target modified appropriately to include the electron density of C_{60}.

This dependence of C_{60} ionization yields on the projectile q_p is in contrast to traditional understanding of ion-atom or ion-solid collision processes. In collisions with thin films, no effect of the projectile q_p is seen on the ionization yields due to the dynamical screening of the projectile nucleus by the diffused valance electron cloud of the solid target. In contrast, ion-atom theories predict a quadratic dependence of single-ionization cross sections on q_p [23]. In Fig. 6, we have plotted the single-ionization cross section for C_{60} along with the CDW-EIS model prediction. CDW-EIS is presently one of the most sophisticated *ab initio* theoretical models for explaining ion-atom collision. As evident from the plot, the linear dependence of the C_{60} single-ionization cross section is in contrast to the nonlinear behavior predicted by the CDW-EIS model. This comparison clearly shows that C_{60} does not behave like other gaseous targets consisting of simple atoms or molecules (such as He, H_2, or Ne). This also reflects that collective effects need to be incorporated in the model to explain the collisional aspects of C_{60}. Kadhane *et al.* [12] have earlier compared the behavior of C_{60} ionization yields with a Ne target and found similar differences. In this regard, the behavior of the fullerene target is somewhat intermediate between atomic gases and bulk systems. It is worth mentioning here that in the present projectile energy range, direct ionization is the dominant process and contributions from electron capture, transfer ionization, etc. are very small [7,13,24], since the projectile velocity (v_p) is much larger than the orbital velocity of target electrons (v_0).

Another interesting feature to note is the smooth behavior of ionization cross sections (see Fig. 5) over projectile ions with different atomic number (Z). In fact one can see that for projectile ions with the same charge state, like C^{5+} and F^{5+} or F^{8+} and Si^{8+}, the ionization cross sections agree within experimental errors. This suggests that projectile nuclear charge does not affect electronic excitations in C_{60}. One may compare these results with the findings of Hadjar *et al.* [2] on C_{60} ionization with low (keV) energy ions. In such low energy collisions, the effect of projectile nuclear charge screening has been known to influence the electronic stopping leading to projectile Z oscillations in ionization cross sections. This kind of effect has also been reported in heavy-ion collisions with thin carbon foils [25]. The projectile Z oscillations are mainly important for low-energy projectile ions where the velocity of the incoming projectile ion is less than the Bohr velocity of the target electrons ($v_p \leqslant v_0$). In our case, the projectile velocity ($v_p \sim 10$ a.u.) is much larger than v_0, and at such short time scales ($\sim 10^{-17}$ s) the contribution from dynamical screening should be very small. Furthermore, due to the high charge state of the projectile ions, very feeble screening of the projectile nucleus is expected in the present case.

V. CONCLUSION

We have investigated the effect of Coulomb perturbation strength of the projectiles on the plasmon excitation in a C_{60} molecule, using fast highly charged heavy ions. For this purpose, the charge states of the projectile ions were varied from 4 to 14 while keeping the velocity of the projectile beam constant. The data were compared with a plasmon excitation model. Qualitatively a reasonable agreement was found between the experimental data and the GDPR model which accounts for about 50% of the single- and double-ionization yields. In fact, the linear dependence of the ionization cross sections on the projectile charge state is very well reproduced by the GDPR model, showing that ionization via plasmon excitation is a dominant channel in a heavy-ion–C_{60} collision. On the other hand, even at the qualitative level, the results were found to be markedly different from the predictions of the CDW-EIS model for single ionization. We also investigated the effect of projectile atomic number on the ionization yields. We did not observe any dependence of the ionization cross sections on the projectile Z. This might be attributed to very feeble screening of the projectile nuclear charge induced by the target electron gas for such highly charged projectile ions and at such short time scales compared to the earlier measurements.

ACKNOWLEDGMENTS

The authors thank the Pelletron accelerator staff for smooth operation of the machine during the experiments.

[1] A. Rudel, R. Hentges, U. Becker, H. S. Chakraborty, M. E. Madjet, and J. M. Rost, Phys. Rev. Lett. **89**, 125503 (2002).
[2] O. Hadjar, R. Hoekstra, R. Morgenstern, and T. Schlatholter, Phys. Rev. A **63**, 033201 (2001).
[3] C. Berchignac and J. P. Connerade, J. Phys. B **27**, 3795 (1994).
[4] G. F. Bertsch, A. Bulgac, D. Tomanek, and Y. Wang, Phys. Rev. Lett. **67**, 2690 (1991).

[5] U. Kadhane, D. Misra, Y. P. Singh, and L. C. Tribedi, Phys. Rev. Lett. **90**, 093401 (2003).
[6] S. Hunsche, T. Starczewski, A. L'Huillier, A. Persson, C. G. Wahlstrom, H. B. van Linden van den Heuvell, and S. Svanberg, Phys. Rev. Lett. **77**, 1966 (1996).
[7] T. LeBrun, H. G. Berry, S. Cheng, R. W. Dunford, H. Esbensen, D. S. Gemmell, and E. P. Kanter, Phys. Rev. Lett. **72**, 3965 (1994).
[8] S. Cheng, H. G. Berry, R. W. Dunford, H. Esbensen, D. S. Gemmell, E. P. Kanter, T. LeBrun, and W. Bauer, Phys. Rev. A **54**, 3182 (1996).
[9] A. Itoh, H. Tsuchida, K. Miyabe, M. Imai, and N. Imanishi, Nucl. Instrum. Methods Phys. Res. B **129**, 363 (1997).
[10] A. Itoh, H. Tsuchida, T. Majima, and N. Imanishi N, Phys. Rev. A **59**, 4428 (1999).
[11] H. Tsuchida, A. Itoh, Y. Nakai, K. Miyabe, and N. Imanishi, J. Phys. B **31**, 5383 (1998).
[12] U. Kadhane, A. Kelkar, D. Misra, A. Kumar, and L. C. Tribedi, Phys. Rev. A **75**, 041201(R) (2007).
[13] A. H. Kelkar, U. Kadhane, D. Misra, A. Kumar, and L. C. Tribedi, J. Phys. B **40**, 2481 (2007).
[14] D. S. F. Crothers and J. F. McCann, J. Phys. B **16**, 3229 (1983).
[15] P. D. Fainstein, V. H. Ponce, and R. D. Rivarola, Phys. Rev. A **45**, 6417 (1992).
[16] W. C. Wiley and I. H. Mclaren, Rev. Sci. Instrum. **26**, 1150 (1955).
[17] A. H. Kelkar, U. Kadhane, D. Misra, A. Kumar, and L. C. Tribedi, Nucl. Instrum. Methods Phys. Res. B **256**, 114 (2007).
[18] J. Abrefah, D. R. Olander, M. Balooch, and W. J. Siekhaus, Appl. Phys. Lett. **60**, 1313 (1992).
[19] D. Misra *et al.*, Nucl. Instrum. Methods Phys. Res. B **267**, 157 (2009).
[20] D. Misra, A. Kelkar, U. Kadhane, A. Kumar, Y. P. Singh, L. C. Tribedi, and P. D. Fainstein, Phys. Rev. A **75**, 052712 (2007).
[21] G. Lapicki and A. R. Zander, Phys. Rev. A **23**, 2072 (1981).
[22] J. Opitz, H. Lebius, B. Saint, S. Jacquet, B. A. Huber, and H. Cederquist, Phys. Rev. A **59**, 3562 (1999).
[23] P. Hvelplund, H. K. Haugen, and H. Knudsen, Phys. Rev. A **22**, 1930 (1980).
[24] H. Knudsen, P. Hvelplund, L. H. Andersen, S. Bjornelund, M. Frost, H. K. Haugen, and E. Samso, Phys. Scr. T **3**, 101 (1983).
[25] P. Hvelplund and B. Fastrup, Phys. Rev. **165**, 408 (1968).